

High-order magneto-hydrodynamic code with spontaneous magnetic fields generation

J. Nikl^{1,2,3}, M. Kuchařík³ and S. Weber¹

¹ ELI Beamlines Centre, Institute of Physics, Czech Academy of Sciences, Czech Republic

² Institute of Plasma Physics, Czech Academy of Sciences, Czech Republic

³ Faculty of Nuclear Sciences and Physical Engineering, Czech Technical University in Prague, Czech Republic



Abstract

The magneto-hydrodynamic description is adopted in many disciplines, where the dynamics of magnetized fluids is investigated. It plays a vital role in plasma physics, where high-temperature plasma becomes highly electrically conductive. Its modelling is then essential for the applications like inertial and magnetic confinement fusion, laboratory astrophysics and many others. For this purpose, we recently developed the resistive magneto-hydrodynamic extension of the multi-dimensional simulation code PETE2 (Plasma Euler and Transport Equations version 2) [1, 2]. The Lagrangian nature of the code means that the computational mesh follows the flow of the matter unlike the traditional codes. Its numerical description is based on the high-order curvilinear finite elements, which provide high precision, computing efficiency, flexibility and robustness. The latest addition is the model of spontaneous magnetic fields, which are generated during the laser–target interaction or at the fronts of cosmic jets and elsewhere. The construction of the code is reviewed and examples of physically relevant simulations are given.

Objectives:

- two-temperature resistive Lagrangian MHD
- high-order curvilinear finite element discretization
- identification and curing of the Biermann catastrophe on shock fronts
- high-order Biermann battery discretization

Lagrangian resistive MHD:

- magnetized fluid in a magnetic field
- resistive electric currents $\vec{j} = \eta^{-1} \vec{E}$ (\vec{E} – fluid-frame electric field, η – resistivity)
- closure model for the stress tensor $\vec{\sigma} = -p\vec{I}$
- magnetic stress tensor $\vec{\sigma}_B = 1/\mu_0(\vec{B}\vec{B} - \frac{1}{2}\vec{B}^2\vec{I})$
- magnetic energy $\epsilon_B = \vec{B}^2/(2\mu_0)$ (in the rest frame)

$$\begin{array}{ll} \text{mass conservation} & \frac{d\rho}{dt} = -\rho\nabla \cdot \vec{u} \\ \text{momentum conservation} & \rho \frac{d\vec{u}}{dt} = \nabla \cdot (\vec{\sigma} + \vec{\sigma}_B) \\ \text{Faraday's law} & \frac{d\vec{B}}{dt} = -\nabla \times \vec{E} \\ \text{internal energy conservation} & \rho \frac{d\epsilon}{dt} = \vec{\sigma} : \nabla \vec{u} + \vec{j} \cdot \vec{E} \\ \text{magnetic energy conservation} & \frac{d\epsilon_B}{dt} = \vec{\sigma}_B : \nabla \vec{u} - \frac{1}{\mu_0} \vec{B} \cdot \nabla \times \vec{E} \end{array}$$

(ρ – mass density, \vec{u} – velocity, ϵ – specific internal en., ϵ_B – specific mag. en., p – pressure)

curvilinear high-order MHD[1]:

- high-order finite elements \Rightarrow computational efficiency, mesh design flexibility
- curvilinear isoparametric finite elements \Rightarrow tracking of interfaces and discontinuities
- mass, momentum and energy conserving
- divergence-free magnetic field
- extended to the two-temperature model[2] for the Biermann battery simulations

functional space name	1D (\parallel / \perp)	2D (\parallel / \perp)	3D
thermodynamic (\mathcal{T})		L_2	
kinematic (\mathcal{K})	$(H^1)^1$	$(H^1)^2$	$(H^1)^3$
magnetic field (\mathcal{M})	$L_2/(L_2)^2$	H_{div}/L_2	H_{div}
electric field (\mathcal{E})	$-(H^1)^2$	H_{curl}/H^1	H_{curl}

Biermann battery

- electron momentum eq. \Rightarrow el. field \vec{E}_B to maintain quasi-neutrality = Biermann term

$$n_e m_e \frac{\partial \vec{u}_e}{\partial t} = 0 = -\nabla p_e - n_e e \vec{E}_B$$

- naive model – direct discretization

$$\vec{E}_B = -\frac{\nabla p_e}{en_e} \quad (\text{pressure is not continuous over a shock front!})$$

- dual form[3] – ideal gas equation-of-state is assumed for $p_e = n_e k_B T_e$ (note gradient parts do not contribute to \vec{B})

$$\vec{E}_B = -\frac{k_B T_e}{e p_e} \nabla p_e = -\frac{k_B}{e} \nabla (T_e \ln p_e) + \frac{k_B \ln p_e}{e} \nabla T_e$$

- spontaneous magnetic field generation

$$\frac{d\vec{B}}{dt} = -\nabla \times \vec{E}_B = -\frac{\nabla n_e \times \nabla p_e}{en_e^2} = \frac{k_B}{e} \nabla \ln p_e \times \nabla T_e$$

- weak formulation (with $\mathcal{G}(\Omega) \subset H_{div}(\Omega)$, $\mathcal{D} \subset L_2(\Omega)$) \Rightarrow high-order FEM discretization

$$\begin{array}{ll} \int_{\Omega} \mathbf{g}_{\ln p_e} \cdot \vec{\xi} dV = \oint_{\partial\Omega} \ln p_e \vec{\xi} \cdot d\vec{S} - \int_{\Omega} \ln p_e \nabla \cdot \vec{\xi} dV & \forall \vec{\xi} \in \mathcal{G}(\Omega) \\ \int_{\Omega} \mathbf{g}_{T_e} \vec{\xi} dV = \oint_{\partial\Omega} T_e \vec{\xi} \cdot d\vec{S} - \int_{\Omega} T_e \nabla \cdot \vec{\xi} dV & \forall \vec{\xi} \in \mathcal{G}(\Omega) \\ \int_{\Omega} \frac{d\vec{B}}{dt} \cdot \vec{\Xi} dV + \int_{\Omega} \alpha \nabla \cdot \vec{\Xi} dV = \frac{k_B}{e} \int_{\Omega} \mathbf{g}_{\ln p_e} \times \mathbf{g}_{T_e} \cdot \vec{\Xi} dV & \forall \vec{\Xi} \in \mathcal{M}(\Omega) \\ \int_{\Omega} \nabla \cdot \mathbf{B} \mu dV = 0 & \forall \mu \in \mathcal{D}(\Omega) \end{array}$$

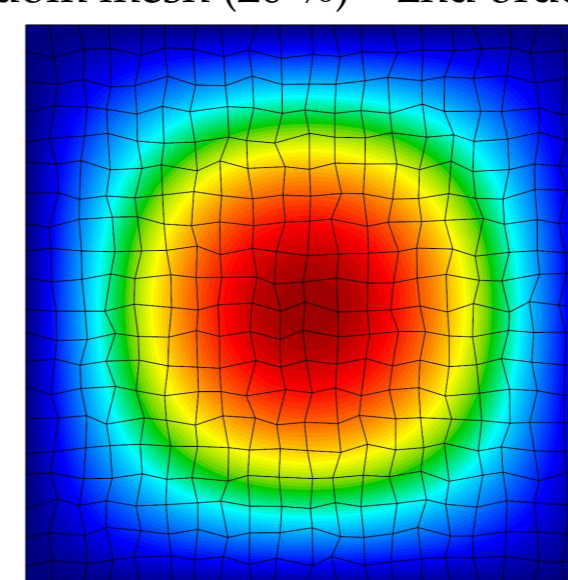
Examples

crossed gradients

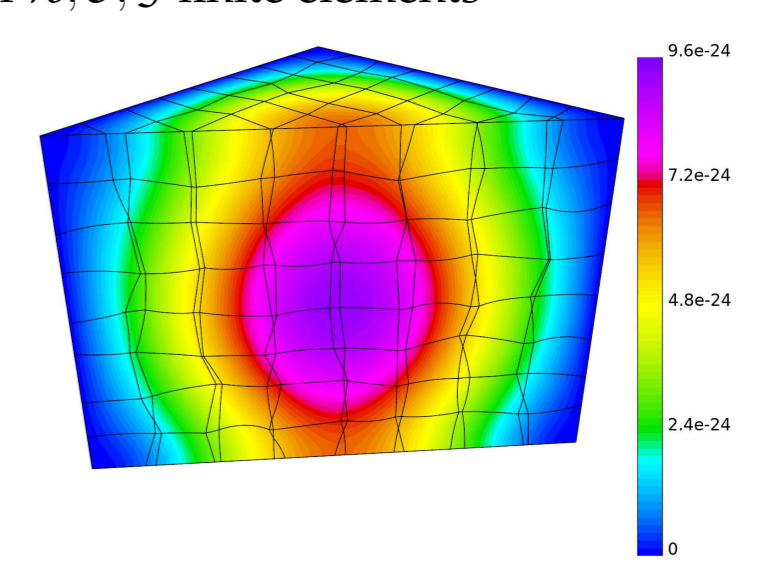
- initial profiles of density and temperature:

$$\begin{array}{l} \rho_0(x, y) = 1 + 10^{-3}(\cos(\pi x) + \cos(\pi y) + \cos(\pi z)) \\ T_0(x, y) = 100 + 10^{-1}(\cos(\pi x) + \sin(\pi y) + \cos(\pi z)) \end{array}$$

- analytic solution for the linear regime ($t = 10^{-20}$ s)
- random mesh (20%) – 2nd order $\mathcal{T}, \mathcal{M}, \mathcal{D}$, 3rd order $\mathcal{K}, \mathcal{E}, \mathcal{G}$ finite elements



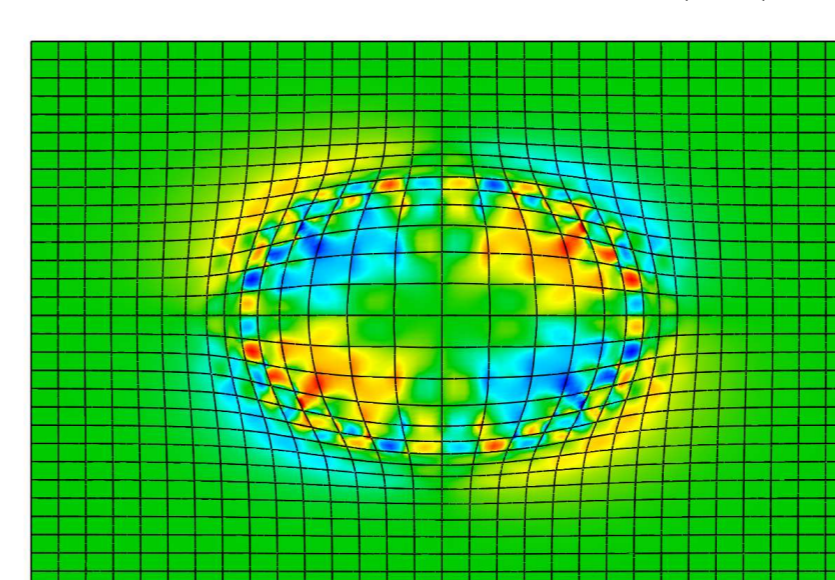
magn. of magnetic field [statT] (20×20 el.)



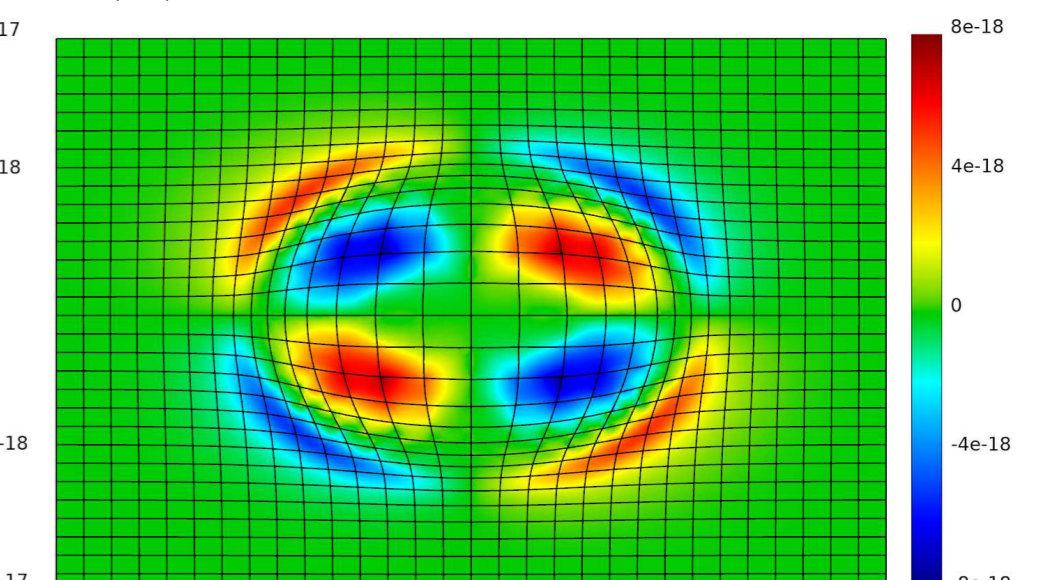
magn. of magnetic field [statT] ($8 \times 8 \times 8$ el.)

ellipsoidal blast wave

- Sedov blast problem for $t < 0.4$ s – high energy placed in the center ($e_0 = 1$ erg) \Rightarrow spherical blast wave to the cold medium ($\gamma = 5/3$, $\rho_0 = 1$ g/cm³, $A = 1$, $Z = 1$)
- domain $\Omega = (-1.5, +1.5) \times (-1.5, +1.5)$ cm
- prolongation of the profiles along the horizontal axis at $t = 0.4$ s by 50 %
- propagation of an ellipsoidal blast wave for 0.4 s $< t \leq 0.6$ s
- heat conduction $\kappa/(\rho c_V e) \doteq 0.35$ cm²/s \Rightarrow crossed gradients of ρ and $T_e \Rightarrow$ generation of \vec{B}
- resistivity $\eta/\mu_0 \doteq 0.018$ cm²/s \Rightarrow slow magnetic field diffusion
- 30×30 elements – 2nd order $\mathcal{T}, \mathcal{M}, \mathcal{D}$, 3rd order $\mathcal{K}, \mathcal{E}, \mathcal{G}$ finite elements



magnetic field – naive [statT]
...totally diverging



magnetic field – dual [statT]
...smooth and convergent

Conclusions

- Biermann battery term constructed for the high-order curvilinear Lagrangian MHD
- two formulations compared on the problem of an ellipsoidal blast wave
- smooth and convergent results obtained for the dual form
- \Rightarrow high-order FE modelling provides high computational efficiency and flexibility
- \Rightarrow enabled detailed simulations of shock-generated magnetic fields in ICF and astrophysics

Forthcoming Research

- generalization for a realistic equation-of-state of electrons
- extension of MHD by additional terms (Nernst effect, Righi-Leduc ...)
- parallelization and optimization for different architectures including IT4I infrastructure

References

- [1] J. Nikl, M. Kuchařík, and S. Weber. High-order curvilinear finite element magneto-hydrodynamics I: A conservative Lagrangian scheme. *Journal of Computational Physics*, 2021. Submitted. arXiv:2110.11669 [physics.comp-ph].
- [2] J. Nikl, M. Kuchařík, M. Holec, and S. Weber. Curvilinear high-order Lagrangian hydrodynamic code for the laser-target interaction. In S. Coda, J. Berndt, G. Lapenta, M. Mantsinen, C. Michaut, and S. Weber, editors, *Europhysics Conference Abstracts – 45th EPS Conference on Plasma Physics*, volume 42A, page P1.2019. European Physical Society, 2018.
- [3] C. Graziani, P. Tzeferacos, D. Lee, D. Q. Lamb, K. Weide, M. Fatenejad, and J. Miller. The Biermann catastrophe in numerical magnetohydrodynamics. *The Astrophysical Journal*, 802(1):43, 2015.

Acknowledgements

Portions of this research were carried out at ELI Beamlines, a European user facility operated by the Institute of Physics of the Academy of Sciences of the Czech Republic. Supported by CAAS project CZ.02.1.01/0.0/0.0/16_019/0000778 from European Regional Development Fund; Czech Technical University grant SGS19/191/OHK4/3T/14 and Czech Science Foundation project 19-24619S. The computations were performed using computational resources funded from the CAAS project. This work has received funding from the Eurofusion Enabling Research Project No. CFP-FSD-AWP21-ENR-01-CEA-02.